Appl. Math. Mech. -Engl. Ed., **41**(12), 1747–1768 (2020)

APPLIED MATHEMATICS AND MECHANICS (ENGLISH EDITION)

https://doi.org/10.1007/s10483-020-2689-9

A review of computational modeling and deep brain stimulation: applications to Parkinson's disease*

Ying YU, Xiaomin WANG, Qishao WANG†, Qingyun WANG

Department of Dynamics and Control, Beihang University, Beijing 100191, China

(Received Oct. 10, 2020 / Revised Oct. 12, 2020)

Abstract Biophysical computational models are complementary to experiments and theories, providing powerful tools for the study of neurological diseases. The focus of this review is the dynamic modeling and control strategies of Parkinson's disease (PD). In previous studies, the development of parkinsonian network dynamics modeling has made great progress. Modeling mainly focuses on the cortex-thalamus-basal ganglia (CTBG) circuit and its sub-circuits, which helps to explore the dynamic behavior of the parkinsonian network, such as synchronization. Deep brain stimulation (DBS) is an effective strategy for the treatment of PD. At present, many studies are based on the side effects of the DBS. However, the translation from modeling results to clinical disease mitigation therapy still faces huge challenges. Here, we introduce the progress of DBS improvement. Its specific purpose is to develop novel DBS treatment methods, optimize the treatment effect of DBS for each patient, and focus on the study in closed-loop DBS. Our goal is to review the inspiration and insights gained by combining the system theory with these computational models to analyze neurodynamics and optimize DBS treatment.

Key words computational model, deep brain stimulation (DBS), Parkinson's disease (PD), basal ganglia (BG)

Chinese Library Classification O175.1
2010 Mathematics Subject Classification 37N25

1 Introduction

Parkinson's disease (PD) is a common chronic neurodegenerative disorder, which involves several neural pathways of motors and non-motors. The core pathology underlying PD is degeneration of dopaminergic neurons in the substantia nigra pars compacta (SNc) in midbrain, leading to the decrease in the dopamine (DA) level in striatum. PD is characterized by motor impairments including rigidity, slowness of movement, and tremor. It can also cause a wide range of non-motor symptoms that appear normally in the course of the disease both early and late-loss of smell, sleep disorders, autonomic dysfunction, cognitive decline, and depression[1]. The severity of these symptoms increases as the PD progresses[2].

* Citation: YU, Y., WANG, X. M., WANG, Q. S., and WANG, Q. Y. A review of computational modeling and deep brain stimulation: applications to Parkinson's disease. *Applied Mathematics and Mechanics* (*English Edition*), **41**(12), 1747–1768 (2020) https://doi.org/10.1007/s10483-020-2689-9

† Corresponding author, E-mail: wangqishao@buaa.edu.cn

Project supported by the National Natural Science Foundation of China (Nos. 11932003 and 11772019)

In PD, the electrophysiologic changes of the basal ganglia (BG), thalamus, and cortex include changes in firing rates, increasing incidence of bursting behaviors, interneuronal synchrony, and enhancing beta-band (13 Hz–35 Hz) oscillatory activity[3–4]. These obvious dynamic changes provide a physiological basis for modeling studies. The lack of DA in the SNc is associated with the pathological dynamics in the motor-related neuronal network spanning the cortico-thalamus- basal ganglia-cortical circuit[5]. Many computational models ranging from the sub-thalamic nucleus (STN)-globus pallidus externa (GPe) circuit, the striatum microcircuit, and basal ganglia-thalamic (BGTH) circuit to the cortex-thalamus-basal ganglia (CTBG) circuit have been proposed in recent years. Even if several advancements in the fields of anatomy, physiology, and biochemistry of these nuclei in BG have yielded new information in the last decades, the molecular and cellular mechanisms involved in the pathogenesis have not been well understood yet. In order to develop effective therapy, the improvement of our current understanding of PD pathogenesis and progression is crucial.

Current treatments aiming at treating motor features help moderate symptomatic effects. However, no available therapy has been proven to be able to cure or slow the process of neurodegeneration[2]. At present, there are mainly three kinds of therapeutic methods to relax symptoms, i.e., medication, surgical procedures, and deep brain stimulation (DBS). DBS is the most common surgical treatment for motor features in advanced PD, though the underlying mechanisms behind DBS remain elusive. The two primary DBS targets are STN and globus pallidus pars interna (GPi). Notably, STN-DBS often results in a greater ability to reduce the need for DA replacement medications and improve the cardinal motor features of PD, while GPi-DBS can reduce motor complications, such as dyskinesia[6]. Although DBS is helpful for the aforementioned motor features, there are still some side effects. The specificity of the patient requires the doctor to spend some time setting the parameters of the neurostimulator, and the battery charging problem is also one of the most common reasons for the pain of DBS patients. Therefore, the improvement of DBS has attracted more and more attention in recent years.

In this review, we shall provide a review of development of a parkinsonian computational model under the new research in the fields of anatomy, physiology, and biochemistry and also a review for recent development of the treatment of PD via DBS, emphasizing the contributions that the system theory has been provided to explain the global dynamics of neuronal circuits which are regulated by DBS. This review highlights the recent improvements in DBS, which may be a significant advancement in the treatment of PD.

2 Computational models of CTBG circuits

The BG is an intricately connected assembly of many subcortical nuclei, forming the core of an adaptive network connecting cortical and thalamic circuits[7–8]. The striatum, GPe, GPi, STN, the substantia nigra pars reticulata (SNr), and SNc are generally considered to be the main components of the BG. The striatum is the main input structure and the principal recipient of cortical inputs and the DA inputs[9], and only two types of neurons are commonly considered in the modeling of striatum, i.e., fast spiking interneuron (FSI) and medium spiny neuron (MSN).

The motor circuit consists of multiple parallel polysynaptic loops, which begins with a convergent input from the cortex to the input nuclei of the BG and then proceeds through different pathways to the GPi or SNr, which projects to the thalamus and the cortex. There are three pathways through the BG, i.e., the direct, indirect, and hyper direct pathways, as depicted in Fig. 1(a). The direct pathway is composed of MSN that expresses DA D1 receptors (D1 MSN), and projects to both SNr and GPi. The indirect pathway is composed of MSN that expresses DA D2 receptors (D2 MSN), and projects to the GPe[10]. The hyper direct pathway is a projection from the cortex to the STN.

In PD, the degeneration and death of dopaminergic neurons in SNc and decrease in the DA level of BG bring about the abnormal function of neural circuitry (see Fig. 1(b)), which also leads to the emergence of the movement disorders and slighter cognitive issues. Albin et al.[11] were the first to put forward the functional explanation for the effects of DA depletion of the BG. The classic model believes that the lack of DA would suppress the D1 MSN projecting to the GPi, and therefore inhibit the direct pathway. Conversely, it would facilitate the activity of the D2 MSN projecting onto the GPe, thus exciting the indirect pathway (see Fig. 1(b)). For striatum microcircuits, DA depletion was implemented by changing the circuit properties. These changes include a reduction in connections between D1 and D2 MSNs, the removement of the connections between D1 MSN, a reduction in mutual inhibition between D2 MSN, and an increase in FSI inhibition to D2 MSN[10]. A result of this effect would be an over-inhibition of the thalamus, which would depress excitatory synapses input in the thalamus to MSNs and cortex.

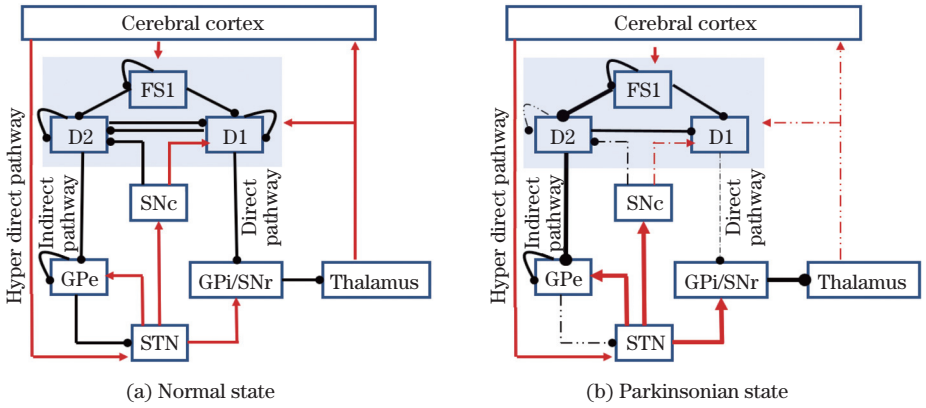

(a) Normal state (b) Parkinsonian state

Fig. 1 CTBG network of (a) normal state and (b) parkinsonian state, where the arrows represent excitatory connections, and the round heads represent inhibitory connection (color online)

At present, even if many advancements in the fields of anatomy, physiology, and biochemistry of these nuclei have yielded new information in the last decades, the internal mechanisms of PD are far to be fully understood. Accordingly, the establishment of reliable computational models to investigate the inner events of the pathogenesis represents a key issue in the field. Current models of neuron and mean-field are predominantly biophysically based and account for several factors that influence the electrophysiology of neurons, e.g., processing of synaptic inputs, ionic basis of electrical excitability, and the effect of DA[12–15]. Here, we review the neuron model and mean-field neural model which are of physiological significance.

2.1 Neural network models

The biological Hodgkin-Huxley (HH) and derivative models have confirmed their availability for recognizing and signifying the electrical activities in single neurons[16–19]. Studies have shown that the CTBG network model for central nervous systems has always been the physiological basis for studying PD. In the past modeling process, the conductivity-based HH model is used to describe the dynamic behavior of different neurons from a mathematical perspective. The HH model is based on the electrical equivalent circuit model which is a useful method to describe the behavior of membrane potential. It mainly includes three parts, i.e., ion channel, power supply, and capacitor. Figure 2(a) shows an equivalent circuit representation of neurons with sodium (Na), calcium (Ca), and potassium (K) ion-channels and leakage current (L). The membrane capacitance current can be expressed as

$$I_{\mathrm{cap}} = C_{\mathrm{m}} \frac{\mathrm{d}V}{\mathrm{d}t}, \tag{1}$$

where C_{m} is the membrane capacitance. In the equivalent circuit, each ion channel is usually represented by a series of conductors. Assume that the conductance of a single ion channel a is g_a. According to Ohm's law, the current of ion channel a can be expressed as

$$I_a = g_a(V - E_a), \tag{2}$$

where E_a is the reversal potential given by the Nernst potential. According to Kirchhoff's current law, the sum of the total current flowing into the cell is zero. The differential equation of membrane potential is obtained as

$$0 = C_{\mathrm{m}}\frac{\mathrm{d}V}{\mathrm{d}t} + \sum_a I_a, \quad a = \{\mathrm{Na}, \mathrm{Ca}, \mathrm{K}, \mathrm{L}\}. \tag{3}$$

Besides, a simple spike model, i.e., the Izhikevich model, reproduces a variety of behaviors of biological neurons, including bursting, spiking, and subthreshold oscillations[20]. It can also be used in the modeling analysis of PD research. Here, we review the computational network models based on a single neuron which has been used in the past few decades, ranging from the BG circuit model, the BGTH model, and the striatum microcircuit model.

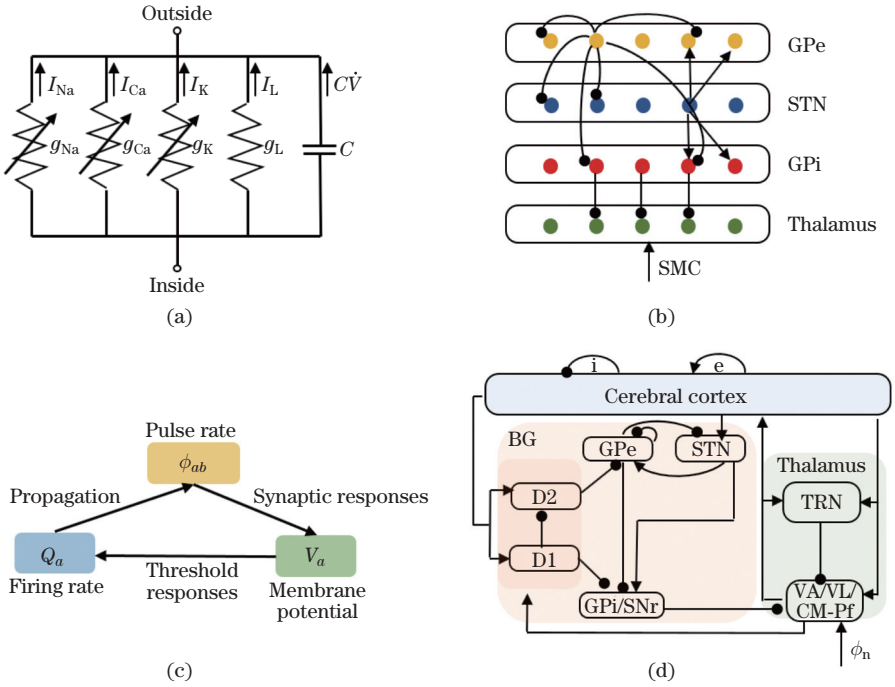

Fig. 2 (a) Equivalent circuit representation of a patch of cell membrane with sodium (Na), calcium (Ca), and potassium (K) ion-channels and leakage current (L); (b) BGTH network connection diagram, where each STN neuron projects to two neighboring GPe and GPi cells, each GPe cell inhibits two neighboring STN, GPe, and GPi cells, each GPi cell inhibits one thalamus cell, and Thalamus receives pulses from the SMC; (c) the conversion relationship among the membrane potential V_a, the mean firing rate Q_a, and the pulse rate ϕ_{ab} in the mean-field model; (d) diagram of the CTBG mean-field model, where the model contains excitatory (denoted by "e") and inhibitory (denoted by "i") interneurons in the cortex, striatum D1, D2 nuclei, GPe, GPi, STN, and the thalamic relay nuclei (TRN) in the thalamus. In addition, the modeling of ventral anterior (VA) nucleus, ventrolateral (VL) thalamic nucleus, and centromedian-parafascicular (CM-Pf) complex is also considered. The arrows represent excitatory glutamate output, and the round heads represent inhibitory GABA output (color online)

Both STN and GPe are the essential components of the indirect pathway in BG, and it is crucial in the motor circuit. The interaction between STN and GPe nucleus is complicated. GPe neurons are excited by the glutamate action of STN neurons, send gamma-aminobutyric acidergic (GABAergic) inhibitory projections to STN, and then are reactivated by the rebound excitatory action of STN[21]. These properties suggest the possibility for intrinsic oscillations arising within the STN-GPe circuit, and therefore capture the dynamic interaction of the STN, and GPe is important to generate the pathological changes in PD. Based on experimental data, Terman et al.[21] established a single-compartment conductance biophysical model of STN and GPe cells, which laid a model foundation for subsequent studies. The dynamics of the neuron membrane potential of STN and GPe can be expressed by the following standardized HH neuron differential equations:

$$C_{\mathrm{m}}V' = -\sum_k I_k^{\mathrm{ion}} - I_{\mathrm{syn}} + I_{\mathrm{app}}, \tag{4}$$

where V is the membrane voltage of STN or GPe, and V' is the derivative of V. I_k^{ion} represents the total ion current of the neuron, and I_{syn} represents the synaptic current. In the network connection between STN and GPe, I_{app} is the bias current acted by peripheral nerve nuclei to adjust the discharge characteristics of different types of neurons. For STN, it includes the potassium current

$$I_{\mathrm{K}} = g_{\mathrm{K}} n^4 (V - E_{\mathrm{K}}),$$

the sodium current

$$I_{\mathrm{Na}} = g_{\mathrm{Na}} m_\infty^3(V) h (V - E_{\mathrm{Na}}),$$

the leakage current

$$I_{\mathrm{L}} = g_{\mathrm{L}} (V - E_{\mathrm{L}}),$$

Ca^{2+} currents

$$I_{\mathrm{T}} = g_{\mathrm{T}} a_\infty^3(V) b_\infty^2(r)(V - E_{\mathrm{Ca}}),$$
$$I_{\mathrm{Ca}} = g_{\mathrm{Ca}} s_\infty^2(V)(V - E_{\mathrm{Ca}}),$$

and a Ca^{2+}-activated after hyperpolarization potassium current

$$I_{\mathrm{AHP}} = g_{\mathrm{AHP}}(V - E_{\mathrm{K}})(C_{\mathrm{Ca}}/(C_{\mathrm{Ca}} + 15)),$$

which depends on the intracellular calcium concentration C_{Ca} to regulate the post-polarization current. The modeling of the ion currents includes different gated variables, which are treated as functions of time and voltage, have the first-order dynamics, and are controlled by the following form of differential equation:

$$\frac{\mathrm{d}X}{\mathrm{d}t} = \varphi_X((X_\infty(V) - X)/\tau_X(V)), \tag{5}$$

where X can be n, h, and r. τ_X is the time constant of ion channel switching. Using this formula, the activation (and deactivation) time constant has an asymmetric bell-shaped relationship with the voltage. The activation gating of the fast activation channel is regarded to be instantaneous. The steady-state voltage dependence can be expressed as $X_\infty(V) = 1/(1+\exp(-(V-\theta_X)/\sigma_X))$, where X can be n, h, a, s, m, or r. The inactivation variable b of T current can be considered as

$$b_\infty(r) = 1/(1 + \exp(-(r - \theta_b)/\sigma_b)) - 1/(1 + \exp(-(-\theta_b)/\sigma_b)),$$

which can make the rebound burst of STN cells more obvious. I_{syn} is mainly the inhibitory effect of GPe on STN, represented by

$$I_{\text{G-S}} = g_{\text{G-S}}(V - V_{\text{G-S}}) \sum s_j,$$

where $g_{\text{G-S}}$ is the maximum synaptic conductivity, and each synaptic variable s_j solves a first-order differential equation as follows:

$$s_j' = \alpha H_\infty(V_{\text{G}j} - \theta_{\text{G}})(1 - s_j) - \beta s_j, \tag{6}$$

where $V_{\text{G}j}$ is the membrane potential of the jth GPe neuron, and

$$H_\infty(V) = 1/(1 + \exp(-(V - \theta_{\text{G}}^H)/\sigma_{\text{G}}^H)).$$

For the modeling of GPe, the synaptic current of GPe includes the excitatory effect of STN on GPe and the inhibitory effect of GPe itself. Terman et al.[21] used each type of network models with 8 to 20 neurons to construct three different structural connections, i.e., random and sparsely connected architecture, structured and sparsely connected architecture, and structured and tightly connected architecture. The results show that the STN-GPe circuit can not only exhibit the rhythmic activity but also have irregular autonomous activity patterns. This provides a basis for explaining the related oscillatory activity in the STN and GPe in PD from a modeling perspective.

GPi is the major output nucleus of BG. Projections of different pathways converge on GPi and then project to thalamus. Simply view the thalamus as a relay station whose role is to respond faithfully to incoming sensorimotor signals, although the function of the thalamus is more than that. A BGTH model by Rubin and Terman[22] provided a mathematical phase plane analysis of the mechanisms that determined thalamic relay capabilities, and introduced the notion of thalamic relay fidelity as a potential indicator of PD for the first time. They considered that GPe and GPi neuron membrane potential dynamics were similar and were expressed by using the same formula. The parameters of the STN model are slightly adjusted to reflect the firing pattern. In addition to BG, the modeling of thalamus neurons simply considers the leakage current, potassium current, sodium current, and T-type current,

$$\begin{cases} C_{\text{m}} V_{\text{TH}}' = -I_{\text{L}} - I_{\text{Na}} - I_{\text{K}} - I_{\text{T}} - I_{\text{G-T}} + I_{\text{SMC}}, \\ h_{\text{T}}' = (h_\infty(V) - h_{\text{T}})/\tau_h(V), \\ r_{\text{T}}' = (r_\infty(V) - r_{\text{T}})/\tau_r(V), \end{cases} \tag{7}$$

where $I_{\text{G-T}}$ is the synaptic current from GPi to thalamus. h_{T} and r_{T} are gated variables. I_{SMC} represents the sensorimotor cortex (SMC) input of the thalamus, and is modeled as a periodic step function of the following form:

$$I_{\text{SMC}} = i_{\text{SMC}} H(\sin(2\pi t/\rho_{\text{SMC}}))(1 - H(\sin(2\pi(t + \delta_{\text{SMC}})/\rho_{\text{SMC}}))). \tag{8}$$

Rubin and Terman[22] established a healthy state and a parkinsonian state by selecting the form of $s(t)$ from GPi to thalamus. The relay capacity of the thalamus can indirectly reflect the state of the system.

Then, the BGTH model was extended and later used to disentangle the contributions of local cells in the subthalamopallidal subsystem and fibers of passage to the modulation of thalamocortical neurons[23]. So et al.[23] improved the model proposed by Rubin and Terman[22]. This modification mainly includes the parameters of the ion channels, the modeling of I_{Ca}, and the synaptic currents. The neuron model qualitatively replicates the firing patterns observed

in experiments. For STN→GPe, STN→GPi, and GPi→TH, the synaptic current is established as

$$\frac{\mathrm{d}s}{\mathrm{d}t} = z, \tag{9}$$

$$\frac{\mathrm{d}z}{\mathrm{d}t} = 0.234u(t) - 0.4z - 0.04s, \tag{10}$$

where $u(t)$ depends on the presynaptic cell potential, when the presynaptic cell crosses the threshold of –10 mV, and $u(t) = 1$. Otherwise, $u(t) = 0$. Figure 2(b) shows the network connection for the BGTH circuit. In the healthy state of the improved BGTH model, the STN, GPe, and GPi neurons present a random discharge pattern, and the thalamic relay neurons can accurately relay the cortical SMC signal input (see Fig. 3(a)). In the parkinsonian state, STN, GPe, and GPi neurons exhibit regular burst oscillations, and thalamic relay neurons

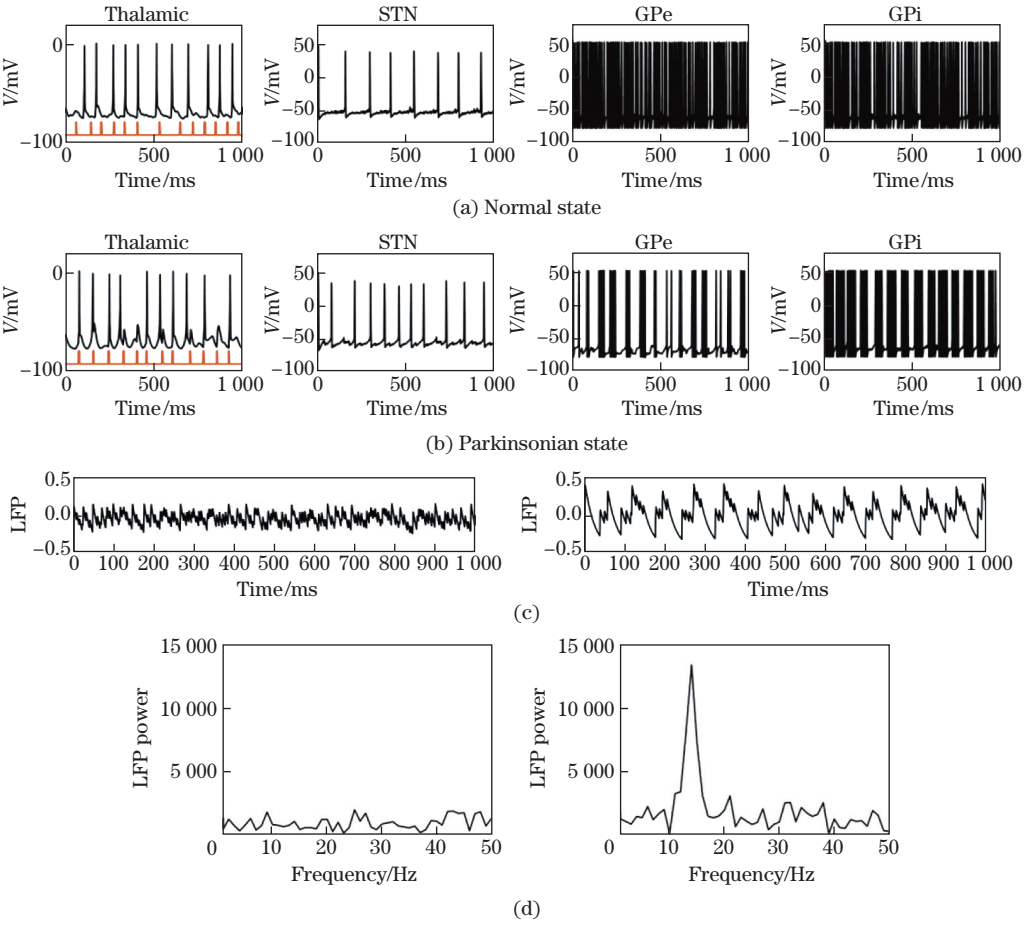

Fig. 3 Firing patterns of GPe, GPi, thalamic, and STN neurons in different states of the BGTH network: (a) normal state, where STN, GPe, and GPi neurons exhibit random firing, and the TRN can accurately relay the cortical SMC signal input; (b) parkinsonian state, where STN, GPe, and GPi neurons exhibit regular cluster oscillations, and TC neurons cannot accurately respond to the cortical SMC signal input; (c) simulating the LFP, compared with the healthy state, in the parkinsonian state, where the amplitude of the LFP is significantly increased due to the increased synchronization between neurons; (d) power spectral density analysis of the LFP under different conditions, in the parkinsonian state, which has an obvious peak in the beta-band (color online)

cannot accurately respond to SMC signal input (see Fig. 3(b)). Besides, they also explore the therapeutic effects of STN-DBS and GPi-DBS. During STN and GPi-DBS, the activation of local cells through fibers reduces thalamic transmission errors. To indirectly reflect the synchronization of neuron groups, it is a good tool to indirectly simulate the local field potential (LFP) by weighting the synaptic variables of neurons (see Subsection 3.2). In the parkinsonian state, the amplitude of LFP increases significantly due to the bursting behavior of neurons (see Fig. 3(c)). Through the power spectral density analysis, it is found that there is an obvious peak in the beta-band which is consistent with the experiment (see Fig. 3(d))[24]. It is worth noting that, in the BGTH model, the striatal inputs to the GPe and GPi are specifically represented by constant currents directly injected into GPe and GPi cells.

The striatum is the main input structure of the BG and receives input from cortex and DA from SNc. Altered firing in the GPe and GPi suggests that striatal MSNs of the direct and indirect pathways are imbalanced during DA depletion. Both MSN classes receive inhibitory input from each other and inhibitory interneurons FSI within the striatum. The effect of DA reduction first appears in the striatum. Therefore, the inhibitory microcircuits of the striatum are known to be critical for motor circuit. There are mainly four types of neurons inside the striatum, of which MSNs account for more than 95%[25]. The modeling of the striatal inhibitory microcircuit is mainly carried out for MSNs and FSIs. Humphries et al.[12] used the Izhikevich model to model DA-modulated MSNs and FSIs. According to different DA receptors, MSNs can be divided into two categories, i.e., D1 MSN and D2 MSN. The relative level of DA receptor occupancy is expressed by the parameter φ_1 (for D1) and parameter φ_2 (for D2) and normalized to the interval [0, 1]. The dynamics of MSNs can be expressed as

$$C_{\mathrm{m}}V'_{\mathrm{D1}} = k(V_{\mathrm{D1}} - V_{\mathrm{r}})(V_{\mathrm{D1}} - V_{\mathrm{t}}) - u + I + \varphi_1 g_{\mathrm{DA}}(V_{\mathrm{D1}} - E_{\mathrm{DA}}), \tag{11}$$

$$C_{\mathrm{m}}V'_{\mathrm{D2}} = k(1 - \alpha\varphi_2)(V_{\mathrm{D2}} - V_{\mathrm{r}})(V_{\mathrm{D2}} - V_{\mathrm{t}}) - u + I, \tag{12}$$

$$I = I_{\mathrm{ampa}} + B(V)I_{\mathrm{nmda}} + I_{\mathrm{gaba\text{-}fs}} + I_{\mathrm{gaba\text{-}ms}}. \tag{13}$$

The formula includes the modulation factor k, the resting and threshold potentials V_{r} and V_{t}, and the synaptic current I. MSNs receive input from the cortex I_{ampa} and I_{nmda}, the inhibitory input $I_{\mathrm{gaba\text{-}fs}}$ from FSI, and the inhibitory input $I_{\mathrm{gaba\text{-}ms}}$ from other MSNs. $B(V)$ simulates the voltage-dependent insertion of magnesium into the N-methyl-D-aspartic acid receptor (NMDA) receptor[12]. FSIs only express the D1 receptor on their cell membrane. Therefore, the membrane potential of FSI can be expressed as

$$C_{\mathrm{m}}V'_{\mathrm{fs}} = k(V_{\mathrm{fs}} - V_{\mathrm{r}}(1 - \eta\varphi_1))(V_{\mathrm{fs}} - V_{\mathrm{t}}) - u_{\mathrm{fs}} + I, \tag{14}$$

$$I = I_{\mathrm{ampa}} + I_{\mathrm{gaba}} + I_{\mathrm{gap}}. \tag{15}$$

According to the experimental results, V_{r} is modulated by $1 - \eta\varphi_1$. The synaptic currents includes the cortical input I_{ampa} and the FSI input I_{gaba}, and there are also electrical synaptic connections inside FSIs. Electrical synaptic connections play a very important role in FSIs. A subsequent study showed that they played a vital role in generating balanced discharges[26]. Based on the above formula, Humphries et al.[12] established a new three-dimensional model of the connectivity of striatal microcircuits, discovered the synchronization behavior within MSNs, and found that the time scale of synchronization largely depends on the simulated DA concentration.

In addition to the modeling with the Izhikevich model, the HH model is also used to model the striatal microcircuit. McCarthy et al.[27] used the HH model to model FSIs and MSNs based on the experimental results. The voltage of each neuron is described as

$$C_{\mathrm{m}}V' = -\sum I_{\mathrm{memb}} - \sum I_{\mathrm{syn}} + I_{\mathrm{app}}. \tag{16}$$

The membrane currents are modeled by HH conductance dynamics

$$I_{\text{memb}} = g(m^n h^k)(V - E_{\text{ion}}),$$

where g is the maximum conductance. E_{ion} stands for the reversal potential. m and h are the activation and inactivation gated variables, respectively. Different from the previous modeling, the MSN neurons contain a special current, i.e., the M-current. The maximum conductance of the M-current is thought to be regulated by acetylcholine in MSNs[27]. By reducing the conductance of the M-current, the characteristics of the striatal network in the parkinsonian state can be indirectly fed back. The simulation results are consistent with the experimental results through an analysis, which indicates that the changes of the M-current conductance and I_{app} modulate the magnitude of the beta oscillation of MSNs[27]. Besides, Wolf[28] used a modified version of the HH formulation to simulate the membrane potential dynamics of MSNs. This model is more complicated and contains dozens of different sodium, potassium, and calcium ion currents, which can replicate many of the responses of these cells to current injection and synaptic input[28]. Subsequently, it has been used to study various dynamic behaviors within striatum[10,26]. The above studies have evaluated the role of the striatal inhibitory circuits in regulating striatum balance.

However, the effects of the striatal inhibitory microcircuits in the BGTH model remain elusive. The striatum involves direct and indirect channels in the classic model. Therefore, it is unwise to ignore the modeling of the striatum to consider parkinsonian dynamics. Kumaravelu et al.[29] developed a biophysical CTBG network model representing the healthy and parkinsonian rat brain, in which the cortical network comprised reciprocally connected regular spiking excitatory neurons and fast-spiking inhibitory interneurons, and striatum modeling took MSNs into account and provided inhibitory input to BG. Recently, Yu and Wang[30] proposed an extended BGTH model containing MSNs and FSIs. The results demonstrated that decreasing the M-current conductance of the MSNs resulted in β-oscillations in the striatum, and increased the inhibition of GPi and GPe by the striatum also caused oscillatory activity in the β-band of BG.

Nevertheless, one caveat with using neuron models is that they increase rapidly in complexity as more neurons and sub-nucleus are modeled, thus making model analyses intractable and having heavy computing burdens. In addition, the parameters of these models are difficult to adjust as they require more data from physiological experiments. Although this neuron model often gives great results in the physiological and clinical sense, it generally lacks some systemic explanation. Therefore, certain researchers have established other types of models to represent and analyze the dynamics of neurons under PD.

2.2 Neural field models

The neuron model focuses on modeling individual neurons with a specific connection structure, and lacks a systematic understanding[31]. When paying attention to the potential dynamics of the BG neural network itself, a different approach, the mean-field model, is used to attempt to simulate population behavior while using fewer dimensions. The mean-field model uses concepts in statistical physics and approximates the more general overall density model, which ignores the interactions between models of a higher order than average activity. It is easier to capture the average electrophysiological activity of a large, spatially distributed neuron collection, thereby enabling a theoretical analysis and extensive simulation of large neural tissue layers.

At present, the mesoscopic model of BG has attracted more and more attention from researchers. As mentioned before, previous studies indicate that the abnormal oscillations in BG may be caused by the interaction between STN and GPe[32–34]. In particular, we introduce the mean-field model of CTBG in detail here. The mean-field model explains not only the dynamic characteristics of the cortex, but also the biological mechanisms of the interaction among cortex, thalamus, and BG, especially the interpretation of PD dynamics. It mainly refers to the

theory proposed by Robinson et al.[35]. Robinson et al.[35] constructed a mean-field model of the cortex-thalamic network, and simulated the normal and epileptic conditions by changing the model parameters. Since motor instructions originate from the cortex, and information flows through the BG to other motor nuclei, it is necessary to study how BG affects the cortical information flow from the perspective of the system and how this effect becomes pathological in PD. The mean-field model system of the CTBG network to study the dynamic behavior of PD was proposed[36–37]. The model contains excitatory (e) and inhibitory (i) interneurons in the cortex, striatum D1, D2 nuclei, GPe, GPi, STN, and TRN in the thalamus (see Fig. 2(d)).

The mean-field model describes the dynamic relationship among the membrane potential, the mean firing rate, and the presynaptic activity of each neuron group (see Fig. 2(c)). For a given nucleus a, the relationship between its mean firing rate Q_a and its corresponding membrane voltage V_a satisfies the similar sigmoidal function as follows:

$$Q_a(r,t) = \frac{Q_a^{\max}}{1+\exp(-(V_a(t)-\theta_a)/\sigma')}, \tag{17}$$

where $Q_a^{\max}$ is the maximum attainable firing rate, r is the spatial position of the nucleus, and θ_a is the mean threshold potential. σ' represents the standard deviation of the threshold. It is usually considered that all the nuclei have the same θ_a value. The dynamics of the mean membrane potential V_a is modeled as

$$D_{\alpha\beta}(t)V_a(t) = \sum_b v_{ab}\varphi_b(t-\tau_{ab}), \tag{18}$$

$$D_{\alpha\beta}(t) = \frac{1}{\alpha\beta}\frac{\mathrm{d}^2}{\mathrm{d}t^2} + \Big(\frac{1}{\alpha}+\frac{1}{\beta}\Big)\frac{\mathrm{d}}{\mathrm{d}t} + 1. \tag{19}$$

Here, $D_{\alpha\beta}$ is a differential operator, which represents the integration of dendrites and synapses of incoming signals. α and β are the reciprocal of the decay and rise time constant of the cell body's response to the input signal, respectively. φ is the input pulse rate, τ_{ab} is the time delay, and v_{ab} is the synaptic strength from the nucleus b to the nucleus a.

For the relationship between φ and Q, Robinson et al.[35] derived a similar attenuation damping wave equation to establish

$$\frac{1}{\gamma_a^2}\Big(\frac{\partial^2}{\partial t^2} + 2\gamma_a\frac{\partial}{\partial t} + \gamma_a^2\Big)\varphi_a(t) = Q_a(t), \tag{20}$$

where γ_a is the damping rate. In practice, we usually think that only the axons of the cortical pyramidal neuron group are long enough to produce significant propagation effects. For other neurons, because the axons are short enough to assume that $\gamma_a = \infty$. In addition, the mean membrane voltage and the firing rate of cortex satisfy $V_{\mathrm{e}} = V_{\mathrm{i}}$ and $Q_{\mathrm{e}} = Q_{\mathrm{i}}$, respectively, which further simplifies the model. The parameters of the CTBG mean-field model within a reasonable range can produce a steady-state discharge rate, and many predictions that have not been mentioned in the previous models are considered. Using the CTBG model, van Albada et al.[36] and van Albada and Robinson[37] deduced the expression of the mean firing rate of each nucleus in a steady state. They simulated DA loss through weaker direct and stronger indirect pathways, which could explain a wide range of electrophysiological phenomena. Besides, they also explored the possible sources of abnormal oscillations in the CTBG, and found that oscillations around 5 Hz and 20 Hz could be generated through a strong indirect way, which would also lead to increase the synchronization of the entire BG.

In addition to exploring PD, the mean-field model of CTBG has also been widely used to explore neurological diseases such as epilepsy[38–39]. Subsequently, based on the mean-field model of CTBG, a new network model for the pedunculopontine nucleus (PPN) was established

to investigate how PPN controls the PD through the projections from the PPN to several key nuclei of BG and thalamus[40]. The results showed that, although PPN stimulation had few effects on the firing rate, it had significant effects on the firing patterns of different nuclei. Most previous brain modeling work has focused on one of these two scales, and the difficulty of compound modeling at the two scales is to create a common representation of neuronal activity[41]. Converting a single spike into an average discharge rate is a direct dimensionality reduction, which can be obtained by averaging the spike activity directly. In contrast, to convert an average population firing rate into a single spike requires additional dimensions. Some studies have proposed a compound spike network/neural field model of the brain. For example, Kerr et al.[41] developed a composite model to explore the effects of driving a spiking network model with several different types of input, including those corresponding to the healthy brain and PD.

The mean-field model has a lower computational burden than the neuron model, and it is a macroscopic model of studying the mechanism of PD, which may understand the role of nuclei in pathophysiology from a more systematic perspective. In parallel with the development of anatomy and physiology, the ability to build computational models to reflect the expanding knowledge of the biophysics of neurons and their networks is maturing at a rapid rate. In the treatment of neurodegenerative disease, DBS treatment for PD is gaining increasing acceptance. Therefore, the integration of control theory, computational neuroscience, and DBS provides an opportunity to create new approaches to the treatment of PD.

3 DBS therapy

DBS is an effective strategy used in the treatment and control of PD[42]. It inserts electrodes into the deep nucleus of the brain and then connects the electrodes to the square wave generator placed in the human subcutaneous tissue with wires to complete the stimulation of parkinsonian patients[43]. The doctor can adjust the frequency, pulse width, or amplitude of the stimulation signal to get the best treatment effect[44–45].

Although DBS is considered to be an effective treatment for PD, its side effects are more obvious. From the system perspective, DBS is an external local control input into the network, which causes several problems. (i) DBS generally uses a single nucleus as the target, and prolonged stimulation will cause specific physical damage[46]. (ii) The battery needs to be replaced by clinical surgery[47–48]. At present, the stimulation frequency required for STN-DBS or GPi-DBS is about 130 Hz–185 Hz[5], and the high energy consumption leads to battery replacement, which will increase the risk of infection in patients. (iii) Due to the lack of adaptation to the needs of patients and the effects of symptoms, doctors need to adjust parameters for a long time to achieve the optimal stimulation effect[44–45]. Therefore, how to improve this inherent treatment strategy and choose a safer and more effective stimulation method is the main problem of the current studies.

3.1 Optimization of DBS: waveform, target, and electrode

In recent years, many studies have proposed that using neuron models improves DBS from different perspectives to reduce stimulation side effects. Improvements to DBS can be divided into three categories (see Fig. 4). The first one is about waveforms. The most commonly used DBS waveform is dominated by rectangular pulse stimulation[22–23,49–50]. Terman et al.[21] modeled this rectangular pulse stimulation as

$$I_{\mathrm{DBS}} = i_{\mathrm{D}} H\Big(\sin\Big(\frac{2\pi t}{\rho_{\mathrm{D}}}\Big)\Big)\Big(1 - H\Big(\sin\Big(\frac{2\pi(t+\delta_{\mathrm{D}})}{\rho_{\mathrm{D}}}\Big)\Big)\Big), \tag{21}$$

where i_{D} is the stimulation amplitude, ρ_{D} is the stimulation period, and δ_D is the duration of each pulse. $H(x)$ represents a Heaviside step function. The HH neuronal network model is usually used to analyze the treatment strategy of DBS. DBS targeting STN and GPi is

considered to be an important form of intervention to relieve PD-related motor symptoms. The DBS is embodied as

$$C_{\mathrm{m}}V' = -\sum_k I_k^{\mathrm{ion}} - I_{\mathrm{syn}} + I_{\mathrm{app}} + I_{\mathrm{DBS}}. \tag{22}$$

The simulation of DBS shows that as the stimulation frequency increases, STN neurons gradually exhibit high-frequency discharges, synchronized with DBS pulses, thus masking the original bursting activity of STN neurons[22–23]. STN activates GPe and GPi neurons through synapse action, causing them to also display high-frequency and regular discharge (see Fig. 5(a)). The application of stimulus changes the firing pattern of neurons and affects the error index (EI) of the thalamic relay. In the modified BGTH model, the relationship between the frequency of EI and DBS is consistent with the clinical observation, that is, the fidelity of the response of thalamic cells is equivalent to that of health, only when the stimulation frequency is greater than 100 Hz[23]. Figure 5(b) shows that EI decreases gradually between 40 Hz and 100 Hz. However, such unbalanced single-phase stimulation currents can damage nerve tissues and cause serious side effects[46]. Therefore, charge-balanced bi-phasic (CBBP) pulses are generally used in actual surgical operations. Fan et al.[46] modeled the CBBP pulse. In order to be consistent with the electrophysiological experiment, a short-duration positive-phase anode pulse of 60 μs was used in each unit stimulation cycle accompanied by a longer-duration negative-phase pulse. $I_{\text{CBBP-DBS}}$ can be considered as

$$I_{\text{CBBP-DBS}} = i_{\mathrm{D}} H_1\Big(H\Big(\sin\Big(\frac{2\pi t}{\rho_{\mathrm{D}}}\Big)\Big)\Big(1 - H\Big(\sin\Big(\frac{2\pi(t+\delta_{\mathrm{D}})}{\rho_{\mathrm{D}}}\Big)\Big)\Big)\Big), \tag{23}$$

where i_{D}, ρ_{D}, δ_{D}, and H are consistent with Eq. (21). H_1 is a bi-valued discrete function,

$$H_1 = \begin{cases} 1, & x = 1, \\ -\dfrac{\delta_{\mathrm{D}}}{\rho_{\mathrm{D}} - \delta_{\mathrm{D}}}, & x = 0. \end{cases} \tag{24}$$

Except for the rectangular pulse, it has been found that special non-rectangular waves may have a better effect on the treatment of PD. Wongsarnpigoon and Grill[51] used the genetic algorithm to calculate the energy-efficient DBS waveform similar to the truncated Gaussian curves, and determined the parameter selection of DBS waveforms. Foutz and Mcintyre[52] evaluated the potential energy savings of non-rectangular stimulation pulses relative to clinical standards. Eight types of stimulation waveforms were considered, i.e., rectangular waveforms, center triangular waveforms, increasing ramp waveforms, decreasing ramp waveforms, increasing exponential waveforms, decreasing exponential waveforms, Gaussian waveforms, and sinusoidal waveforms (see Fig. 4(a))[52]. Studies have shown that the use of non-rectangular stimulation waveforms can save up to 64% of energy. The delay time between the cathode and anode parts of the charge balance Gaussian waveform is proposed to desynchronize the GPe and GPi neurons[53]. The amount of energy consumed by Gaussian Delay Gaussian (GDG) waveforms is 60% lower than a rectangular charged balanced pulse[53]. Recently, noise stimulation has been used to destroy the firing pattern of pathological neuronal activity[54]. Compared with the traditional DBS paradigm, low-frequency and low-intensity noise stimulation with balanced waveforms can reduce the energy consumption of the stimulation by 50%.

The second one is to improve the target. Through the study of the BG, it is found that the parkinsonian motor dysfunction is closely related to STN and GPi neurons[55–56]. Therefore, STN and GPi are used as common targets of DBS, and a series of results have been obtained. Recently, it was reported that GPe-DBS changed the firing patterns of STN, GPi, and thalamic neurons in PD monkeys, and improved abnormal motor signals, suggesting that GPe may

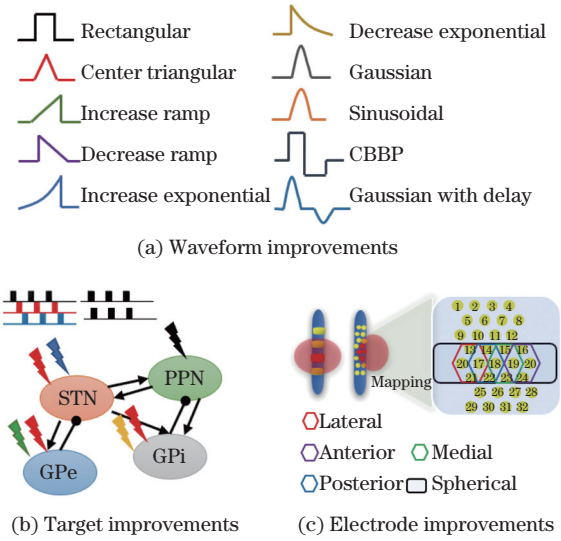

Fig. 4 (a) Waveform improvements, where rectangular waveforms, center triangular waveforms, increasing ramp waveforms, decreasing ramp waveforms, increasing exponential waveforms, decreasing exponential waveform, Gaussian waveform, sinusoidal waveform, CBBP pulses waveform, and Guassian with delay waveform are considered[46,51,57]; (b) target waveforms; (c) electrode improvements, consistent with the process of the experiment[58], where five adjacent contacts were selectively extracted and activated to generate different stimulation fields, such as the front, back, outer, and middle sides of the STN[46] (color online)

become a target of DBS[59]. In terms of targets, there are two different types of stimulation, i.e., multi-site stimulation and multi-target stimulation. From the perspective of modeling, Tass[60–61] proposed that perfect desynchronization could be achieved by stimulating all neurons individually, and each neuron had its own electrode and its own reset stimulation. However, each neuron had its electrode, which will damage the tissue. Thus, it is not feasible. The individual control mode can be approximated by stimulation at multiple sites, where such stimulation can be achieved by the neural chip technique[62]. They proposed coordinated reset (CR) stimulation, which is a desynchronized stimulation technique based on the coordinated phase reset of each subgroup of the synchronized nervous system[63]. The stimulation signal is managed in a time coordinated manner through the stimulation site so that the next stimulation site is delayed after the previous stimulation site is activated. Lysyansky et al.[64] also optimized CR stimulation to minimize the total amount of stimulation current required, depending on the stimulus intensity and stimulus sequence parameters, including the length of the stimulus program on and off. For example, CR is applied in the m:n switch mode, where m cycles with CR are followed by n cycles without any stimulation[64]. Stimulation has a significant desynchronization effect while minimizing the total amount of stimulation current delivered. The other is multi-target stimulation. Fan and Wang[65] used the BGTH model to explore the effects of multi-target stimulation on PD. The microelectrodes are placed in three different nuclei of STN, GPe, and GPi, and high-frequency pulse stimulation currents are alternately injected into different nuclei. Recently, Yu et al.[66] proposed the combined DBS of two nuclei (CDBS), which is to inject two kinds of low-frequency pulse stimulation currents with phase difference by placing two microelectrodes in the BG. Under certain parameters, the energy consumption of CDBS is reduced by 70% compared with high-frequency DBS, and the stimulation frequency is reduced to about 40 Hz. Figure 5(c) shows the changes of the raster patterns of STN, GPe, and GPi neurons under the CDBS. The phenomenon of bursting synchronous discharge in the parkinsonian state has been significantly improved. This control method can alternately

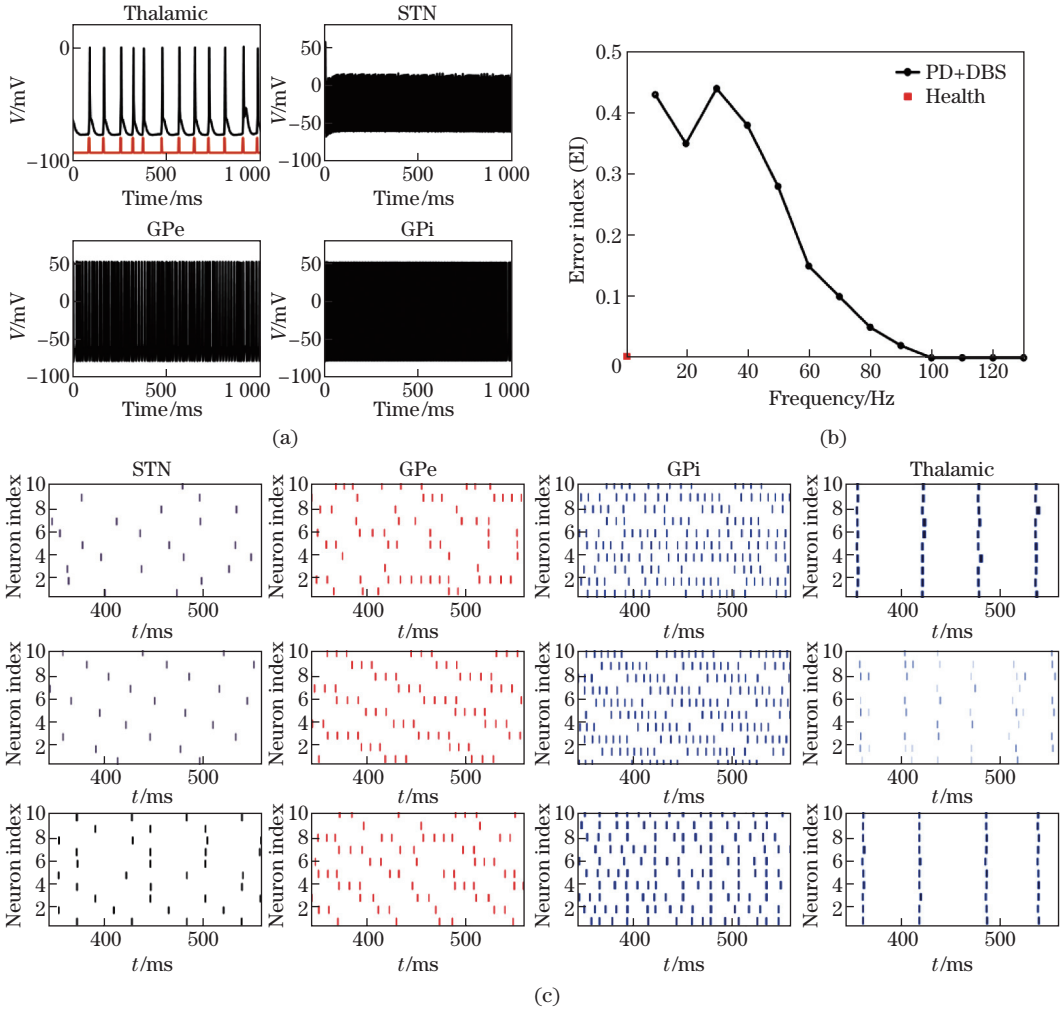

Fig. 5 (a) 120 Hz STN-DBS, STN, and GPi neurons exhibit high-frequency firing patterns, and the thalamus also resumes its normal ability to relay SMC signals; (b) the reliability level of thalamus neurons in response to cortical SMC signal input varies with stimulation frequency[23]; (c) an example of dual-target joint stimulation which can desynchronize the neuron group, from top to bottom: healthy state, pathologic state, and CDBS[66] (color online)

stimulate multiple subcutaneous structures, thus effectively reducing the physical damage caused by long-lasting stimulation of a single site. In addition to the BG, in recent years, studies have found that PPN is closely related to the axial symptoms in patients with advanced PD[67–69]. Many clinical studies have shown that low-frequency stimulation of PPN can also improve the axial symptoms of PD[67].

The traditional stimulation electrode has four longitudinally arranged cylindrical contacts, which have a large contact area and weak controllability[70]. To obtain the best clinical effect, it is necessary to maximize the coverage of the area while minimizing the spread of current to adjacent structures to avoid adverse side effects. Martens et al.[70] used a computational model to simulate the voltage distribution and DBS activation volume. The electrodes arranged in a cylindrical array can direct the stimulation field to the main direction field. Contarino et al.[58] developed a direction-controllable DBS electrode with 32 contacts that can effectively control the direction and range of the stimulation field. Fan et al.[46] used the BGTH model, combined with related electrophysiological experiments and anatomical characteristics, to verify

that STN's four different directions of stimulation had better control effects in improving neuronal cluster desynchronization. They selected four sets of contact sets (each set of contact sets consists of four adjacent contacts) to represent four directional stimulus strategies, i.e., anterior, posterior, lateral, and medial. If the contacts surrounded by the rounded rectangle are activated at the same time, a spherical stimulation field for STN will be generated (see Fig. 4(c)). Numerical simulations show that the reliability level of thalamus neurons in response to cortical SMC signal input varies with stimulation intensity[46]. Through the analysis, it can be seen that there is at least one directional control stimulus that can make the relay ability of TC neurons decrease faster than the spherical stimulation mode within a specific stimulation intensity range. The improvement work on DBS is still in progress and is expected to be further applied to the clinical treatment.

3.2 Closed loop DBS

The electrodes of DBS are usually permanently implanted in the BG, and the stimulator delivers electrical impulses continuously and independently, without relying on any feedback (open-loop stimulation). On the contrary, in closed-loop stimulation, electrical stimulation is delivered as a function of neuronal activity, which is adjusted in real-time[71]. Demand-based closed-loop feedback control is smarter than the normal DBS and avoids harmful side effects caused by constant stimulation[72]. It can maximize the treatment effect while minimizing the amount of stimulation and the time to adjust stimulation settings.

Closed-loop stimulation methods mainly include two types. The first type method uses the high-frequency DBS waveform, and adjusts the stimulation parameters through closed-loop control. The second type method can be considered as a "mild stimulation", which attempts to adjust the pathological oscillation network in an on-demand manner[73]. Regarding the feedback signal of closed-loop stimulation, we usually use the LFP of STN in modeling[74]. In clinical experiments, it can be recorded from the end of the electrode used for DBS. Studies have shown that the LFP is closely related to the activity of individual neurons and shows obvious β-band oscillations in the PD state[74]. The amplitude of the filtered LFP can indirectly reflect the degree of synchronization of neurons (see Fig. 3(c)). Generally, in the neuronal network model, to calculate the magnitude of the stimulus signal, the LFP is modeled, which is related to the average synaptic activity of the neuron,

$$P_{\mathrm{LF}} = N^{-1} \sum_{j=1}^{N} s_j, \tag{25}$$

where $s_j(t)$ is the synaptic variable which is consistent with Eq. (6). Then, filter the LFP of STN by applying a linear damped oscillator as follows:

$$\ddot{u} + \alpha_{\mathrm{d}} \dot{u} + \omega^2 u = k_{\mathrm{f}} P_{\mathrm{LF}}(t), \tag{26}$$

where

$$\omega = 2\pi/T,$$

in which T is the period of LFP. α_{d} and k_{f} are constants used to maintain the amplitude of the input original LFP signal. The amplitude of the filtered LFP signal can indirectly reflect the strong and weak synchronization state of neurons. The stimulation is modulated by the linear delay feedback method as follows:

$$I_{\mathrm{stim}} = K(x(t-\tau) - x(t)), \tag{27}$$

where $x(t) = \dot{u}$, and K is the stimulation intensity[75]. Popovych and Tass[75] found that modulating the amplitude of pulsed high-frequency stimulation through linear or nonlinear delay feedback methods could effectively and robustly desynchronize the STN-GPe network model.

Furthermore, they proposed a pulsed multi-site linear feedback control, considering 200 STN neurons and adding four stimulation sites, which could achieve a more effective desynchronization effect. Guo and Rubin[76] used a computational model of the BGTH to explore a multi-site delayed feedback stimulation (MDFS), which filtered the simulated LFP signal to generate a stimulus signal. A new frequency adaptive stimulation control strategy based on the LFP in the closed-loop model was proposed[77]. For example, high-frequency stimulation is only triggered at the peak of the filtered LFP (see Fig. 6(b)). Besides, Su et al.[78] systematically studied the modulation of the amplitude, frequency, and pulse width of the DBS signal through closed-loop stimulation. The closed-loop adjustment of the DBS parameters shows better desynchronization and is also energy-efficient.

Adaptive DBS (aDBS) is also a closed-loop system, which changes the stimulation parameters in real time according to the patient's clinical status to provide treatment for patients with movement disorders. The aDBS uses feedback about the state of the neural circuit to control the stimulus, instead of providing a fixed stimulus as before[79–81]. Little et al.[80] conducted a systematic test on the aDBS in PD clinical trials. Stimulation was only turned on when the β-amplitude was higher than the preset threshold, while it was turned off when the amplitude was lower than the preset threshold. Compared with traditional DBS, aDBS is far more effective (absolutely reduced by 27%), and the stimulation time is reduced by 56%[79]. Recently, Velisar et al.[82] proposed a new dual-threshold algorithm, which used a dual-threshold strategy for the β-activity of STN to change the stimulation voltage. In addition, an improved DBS algorithm was implemented using classic traditional proportional-integral-derivative (PID) methodology[83]. For example, the control based on the reliability of the thalamus adopts a proportional control strategy to achieve optimal control under a given energy consumption. Closed-loop stimulation is more adaptable than open-loop stimulation. Based on theoretical modeling results, the maximum effectiveness of different closed-loop parameters in human PD patient experimental models needs further study.

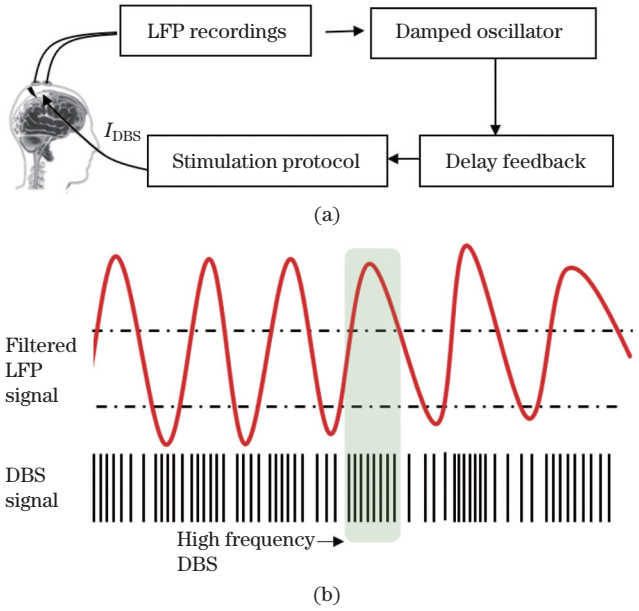

Fig. 6 Feedback loop: (a) the LFP signal of STN is recorded and then filtered with a damped oscillator, and the result is shifted through a linear or nonlinear delayed feedback and then through the special stimulation protocol to produce the DBS signal; (b) an example of the LFP amplitude adjusting the frequency of the stimulation signal (color online)

4 Summary and outlook

We systematically summarize the dynamic modeling analysis and control strategies related to PD in recent decades. According to the records and analysis of clinical experiments, the nucleus within the BG in the parkinsonian network exhibits bursting a discharge behavior, and the synchronization level increases. Through the power spectral density analysis, it is found that the energy of STN and GPi nucleus increases significantly in the beta-band. Using the neuron model and the field model, these dynamic characteristics are well reflected. Models are generally based on CTBG circuits. Except for the striatum, we generally consider other nuclei as a whole in modeling. Recently, optogenetics has been used to specifically stimulate the neuron population in GPe[84], where targeted interventions reliably induce long-term exercise rescue in PD mouse models. Studies have developed molecular and genetic strategies to subdivide GPe neurons into subgroups, which have different physiological and anatomical projections[85–86]. In the prototype population, neurons can be further subdivided according to the expression of parvalbumin (PV)-GPe and Lim homeobox 6 (Lhx6)-GPe[85–86]. The long-lasting recovery of the movement of PD mice can be achieved by selective excitatory stimulation of PV-GPe or inhibitory stimulation of Lhx6-GPe[84]. Therefore, the identification of different cell types in the BG is essential for us to understand the function of the BG and treat neurological disorders, especially PD. At present, in terms of modeling study, the specific modeling of the nucleus within the BG is blank, which will be an important node for subsequent study. Because certain dynamic effects are only achieved by limiting the operation of specific neuron subgroups, rather than by regulating all neurons at the same time. The specific modeling of neurons helps us to further understand the dynamic mechanism of PD[5].

At present, the computational model has been widely used to find more novel, irregular, and low-frequency DBS strategies, and the results obtained are generally more energy-efficient than traditional DBS. In order to solve the problem of higher damage to a single target, the multi-target stimulation strategy is proposed. However, the current study on targets mostly stays on the structure of the BG. Simulating complex neural networks provides a unique opportunity to evaluate new stimulation targets. It is necessary to explore more effective stimulation targets. In addition, to reduce the adjustment time of DBS, many studies have combined model-based control techniques to design a closed-loop aDBS strategy. However, the improvement of DBS seems to be a huge project, the clinical application is not abundant, and there are still considerable differences between the models and the actual applications. In general, these solutions are still in the early theoretical stage, and it takes a long time to transition from the preclinical trial stage to the clinical trial stage[5].

In addition to electrical stimulation, optogenetic stimulation is slowly emerging for the regulation of neurons. This technique can control neural activity in a cell-specific way with a high degree of time accuracy, which is a significant advantage over traditional techniques such as electrical stimulation[87]. Optogenetic stimulation combines genetic and optical tools to stimulate specific neurons. Electrical stimulation will drive the activity of all cells in the area where the electrode is located through the coupling relationship between neurons[88], including some axons in the cell body far away from the target[89]. These compound effects may make it difficult to understand the stimulus and may lead to off-target adverse effects. Optogenetic stimulation is aimed at specific cell types. It is potentially highly spatially selective, and external stimuli can have no direct contact with cells[87]. Neuron optogenetic tools can also be divided into excitatory and inhibitory[89]. Therefore, it can tell us more specifically whether the effect on neurons is excitatory or inhibitory. Therefore, we can use optogenetic stimulation to explore the therapeutic mechanism of DBS, which can be further used to understand the mechanism of PD and improve electrical DBS.

References

[1] DORSEY, E., SHERER, T., OKUN, M., and BLOEM, B. The rise of Parkinson's disease. *American Scientist*, **108**, 176 (2020)

[2] DEXTER, D. T. and JENNER, P. Parkinson disease: from pathology to molecular disease mechanisms. *Free Radical Biology and Medicine*, **62**, 132–144 (2013)

[3] GALVAN, A. and WICHMANN, T. Pathophysiology of parkinsonism. *Clinical Neurophysiology*, **119**, 1459–1474 (2008)

[4] RUBIN, J. E., MCINTYRE, C. C., TURNER, R. S., and WICHMANN, T. Basal ganglia activity patterns in parkinsonism and computational modeling of their downstream effects: basal ganglia activity patterns in parkinsonism. *European Journal of Neuroscience*, **36**, 2213–2228 (2012)

[5] SANTANIELLO, S., GALE, J. T., and SARMA, S. V. Systems approaches to optimizing deep brain stimulation therapies in Parkinson's disease. *WIREs Systems Biology and Medicine*, **10**, e1421 (2018)

[6] JAKOBS, M., LEE, D. J., and LOZANO, A. M. Modifying the progression of Alzheimer's and Parkinson's disease with deep brain stimulation. *Neuropharmacology*, **171**, 107860 (2020)

[7] PLOTKIN, J. L. and GOLDBERG, J. A. Thinking outside the box (and arrow): current themes in striatal dysfunction in movement disorders. *Neuroscientist*, **25**, 359–379 (2019)

[8] BAR-GAD, I., MORRIS, G., and BERGMAN, H. Information processing, dimensionality reduction and reinforcement learning in the basal ganglia. *Progress in Neurobiology*, **71**, 439–473 (2003)

[9] MALLET, N., DELGADO, L., CHAZALON, M., MIGUELEZ, C., and BAUFRETON, J. Cellular and synaptic dysfunctions in Parkinson's disease: stepping out of the striatum. *Cells*, **8**, 1005 (2019)

[10] DAMODARAN, S., CRESSMAN, J. R., JEDRZEJEWSKI-SZMEK, Z., and BLACKWELL, K. T. Desynchronization of fast-spiking interneurons reduces-band oscillations and imbalance in firing in the dopamine-depleted striatum. *Journal of Neuroscience*, **35**, 1149–1159 (2015)

[11] ALBIN, R. L., YOUNG, A. B., and PENNEY, J. B. The functional anatomy of basal ganglia disorders. *Trends in Neurosciences*, **12**, 366–375 (1989)

[12] HUMPHRIES, M. D., WOOD, R., and GURNEY, K. Dopamine-modulated dynamic cell assemblies generated by the GABAergic striatal microcircuit. *Neural Networks*, **22**, 1174–1188 (2009)

[13] MANDALI, A., RENGASWAMY, M., CHAKRAVARTHY, V. S., and MOUSTAFA, A. A. A spiking basal ganglia model of synchrony, exploration and decision making. *Frontiers in Neuroscience*, **9**, 191 (2015)

[14] BAHUGUNA, J., AERTSEN, A., KUMAR, A., and BLACKWELL, K. T. Existence and control of go/no-go decision transition threshold in the striatum. *PLoS Computational Biology*, **11**, e1004233 (2015)

[15] MUDDAPU, V. R., MANDALI, A., CHAKRAVARTHY, V. S., and RAMASWAMY, S. A computational model of loss of dopaminergic cells in Parkinson's disease due to glutamate-induced excitotoxicity. *Frontiers in Neural Circuits*, **13**, 11 (2019)

[16] HODGKIN, A. L. and HUXLEY, A. F. A quantitative description of membrane current and its application to conduction and excitation in nerve. *Bulletin of Mathematical Biology*, **52**, 25–71 (1990)

[17] MA, J. and TANG, J. A review for dynamics in neuron and neuronal network. *Nonlinear Dynamics*, **89**, 1569–1578 (2017)

[18] MA, J., YANG, Z., YANG, L., and TANG, J. A physical view of computational neurodynamics. *Journal of Zhejiang University-Science A*, **20**, 639–659 (2019)

[19] WANG, W. and WANG, R. Control strategy of central pattern generator gait movement under condition of attention selection. *Applied Mathematics and Mechanics* (*English Edition*), **37**(7), 957–966 (2016) https://doi.org/10.1007/s10483-016-2096-9

[20] IZHIKEVICH, E. M. Simple model of spiking neurons. *IEEE Transactions on Neural Network*, **14**, 1569–1572 (2003)

[21] TERMAN, D., RUBIN, J. E., YEW, A. C., and WILSON, C. J. Activity patterns in a model for the subthalamopallidal network of the basal ganglia. *Journal of Neuroscience*, **22**, 2963–2976 (2002)

[22] RUBIN, J. E. and TERMAN, D. High frequency stimulation of the subthalamic nucleus eliminates pathological thalamic rhythmicity in a computational model. *Journal of Computational Neuroscience*, **16**, 211–235 (2004)

[23] SO, R. Q., KENT, A. R., and GRILL, W. M. Relative contributions of local cell and passing fiber activation and silencing to changes in thalamic fidelity during deep brain stimulation and lesioning: a computational modeling study. *Journal of Computational Neuroscience*, **32**, 499–519 (2012)

[24] BROWN, P. and WILLIAMS, D. Basal ganglia local field potential activity: character and functional significance in the human. *Clinical Neurophysiology*, **116**, 2510–2519 (2005)

[25] KREITZER, A. C. Physiology and pharmacology of striatal neurons. *Annual Review of Neuroscience*, **32**, 127–147 (2009)

[26] DAMODARAN, S., EVANS, R. C., and BLACKWELL, K. T. Synchronized firing of fast-spiking interneurons is critical to maintain balanced firing between direct and indirect pathway neurons of the striatum. *Journal of Neurophysiology*, **111**, 836–848 (2014)

[27] MCCARTHY, M. M., MOORE-KOCHLACS, C., GU, X., BOYDEN, E. S., HAN, X., and KOPELL, N. Striatal origin of the pathologic beta oscillations in Parkinson's disease. *Proceedings of the National Academy of Sciences*, **108**, 11620–11625 (2011)

[28] WOLF, J. A. NMDA/AMPA ratio impacts state transitions and entrainment to oscillations in a computational model of the nucleus accumbens medium spiny projection neuron. *Journal of Neuroscience*, **25**, 9080–9095 (2005)

[29] KUMARAVELU, K., BROCKER, D. T., and GRILL, W. M. A biophysical model of the cortex-basal ganglia-thalamus network in the 6-OHDA lesioned rat model of Parkinson's disease. *Journal of Computational Neuroscience*, **40**, 207–229 (2016)

[30] YU, Y. and WANG, Q. Oscillation dynamics in an extended model of thalamic-basal ganglia. *Nonlinear Dynamics*, **98**, 1065–1080 (2019)

[31] CAIOLA, M. and HOLMES, M. H. Model and analysis for the onset of parkinsonian firing patterns in a simplified basal ganglia. *International Journal of Neural, Systems*, **29**, 1850021 (2019)

[32] GILLIES, A., WILLSHAW, D., and LI, Z. Subthalamic-pallidal interactions are critical in determining normal and abnormal functioning of the basal ganglia. *Proceedings of the Royal Society B: Biological Science*, **269**, 545–551 (2002)

[33] HOLGADO, A. J. N., TERRY, J. R., and BOGACZ, R. Conditions for the generation of beta oscillations in the subthalamic nucleus-globus pallidus network. *Journal of Neuroscience*, **30**, 12340–12352 (2010)

[34] PLENZ, D. and KITAL, S. T. A basal ganglia pacemaker formed by the subthalamic nucleus and external globus pallidus. *nature*, **400**, 677–682 (1999)

[35] ROBINSON, P. A., RENNIE, C. J., and ROWE, D. L. Dynamics of large-scale brain activity in normal arousal states and epileptic seizures. *Physical Review E*, **65**, 041924 (2002)

[36] VAN ALBADA, S. J., GRAY, R. T., DRYSDALE, P. M., and ROBINSON, P. A. Mean-field modeling of the basal ganglia-thalamocortical system II. *Journal of Theoretical Biology*, **257**, 664–688 (2009)

[37] VAN ALBADA, S. J. and ROBINSON, P. A. Mean-field modeling of the basal ganglia-thalamocortical system I. *Journal of Theoretical Biology*, **257**, 642–663 (2009)

[38] CHEN, M., GUO, D., WANG, T., JING, W., XIA, Y., XU, P., LUO, C., VALDES-SOSA, P. A., and YAO, D. Bidirectional control of absence seizures by the basal ganglia: a computational evidence. *PLoS Computational Biology*, **10**, e1003495 (2014)

[39] FAN, D., ZHENG, Y., YANG, Z., and WANG, Q. Improving control effects of absence seizures using single-pulse alternately resetting stimulation (SARS) of corticothalamic circuit. *Applied Mathematics and Mechanics* (*English Edition*), **41**(9), 1287–1302 (2020) https://doi.org/10.1007/s10483-020-2644-8

[40] YU, Y., ZHANG, H., ZHANG, L., and WANG, Q. Dynamical role of pedunculopntine nucleus stimulation on controlling Parkinson's disease. *Physica A: Statistical Mechanics and Its Applications*, **525**, 834–848 (2019)

[41] KERR, C. C., VAN ALBADA, S. J., NEYMOTIN, S. A., CHADDERDON, G. L., ROBINSON, P. A., and LYTTON, W. W. Cortical information flow in Parkinson's disease: a composite network/field model. *Frontiers in Computational Neuroscience*, **7**, 39 (2013)

[42] FASANO, A., APPEL-CRESSWELL, S., JOG, M., ZUROWKSKI, M., DUFF-CANNING, S., COHN, M., PICILLO, M., HONEY, C. R., PANISSET, M., and MUNHOZ, R. P. Medical management of Parkinson's disease after initiation of deep brain stimulation. *Canadian Journal of Neurological Sciences*, **43**, 626–634 (2016)

[43] HICKEY, P. and STACY, M. Deep brain stimulation: a paradigm shifting approach to treat Parkinson's disease. *Frontiers in Neuroscience*, **10**, 173 (2016)

[44] BENABID, A. L., CHABARDES, S., MITROFANIS, J., and POLLAK, P. Deep brain stimulation of the subthalamic nucleus for the treatment of Parkinson's disease. *The Lancet Neurology*, **8**, 67–81 (2009)

[45] PICILLO, M., LOZANO, A. M., KOU, N., PUPPI MUNHOZ, R., and FASANO, A. Programming deep brain stimulation for Parkinson's disease: the Toronto western hospital algorithms. *Brain Stimulation*, **9**, 425–437 (2016)

[46] FAN, D., WANG, Z., and WANG, Q. Optimal control of directional deep brain stimulation in the parkinsonian neuronal network. *Communications in Nonlinear Science and Numerical Simulation*, **36**, 219–237 (2016)

[47] WEI, X. F. and GRILL, W. M. Impedance characteristics of deep brain stimulation electrodes in vitro and in vivo. *Journal of Neural Engineering*, **6**, 046008 (2009)

[48] BUTSON, C. R. and MCINTYRE, C. C. Current steering to control the volume of tissue activated during deep brain stimulation. *Brain Stimulation*, **1**, 7–15 (2008)

[49] MORO, E., ESSELINK, R. J. A., XIE, J., HOMMEL, M., BENABID, A. L., and POLLAK, P. The impact on Parkinson's disease of electrical parameter settings in STN stimulation. *Neurology*, **59**, 706–713 (2002)

[50] PIRINI, M., ROCCHI, L., SENSI, M., and CHIARI, L. A computational modelling approach to investigate different targets in deep brain stimulation for Parkinson's disease. *Journal of Computational Neuroscience*, **26**, 91–107 (2009)

[51] WONGSARNPIGOON, A. and GRILL, W. M. Energy-efficient waveform shapes for neural stimulation revealed with a genetic algorithm. *Journal of Neural Engineering*, **7**, 046009 (2010)

[52] FOUTZ, T. J. and MCINTYRE, C. C. Evaluation of novel stimulus waveforms for deep brain stimulation. *Journal of Neural Engineering*, **7**, 066008 (2010)

[53] DANESHZAND, M., FAEZIPOUR, M., and BARKANA, B. D. Computational stimulation of the basal ganglia neurons with cost effective delayed Gaussian waveforms. *Frontiers in Computational Neuroscience*, **11**, 73 (2017)

[54] LIU, C., WANG, J., DENG, B., LI, H., FIETKIEWICZ, C., and LOPARO, K. A. Noise-induced improvement of the parkinsonian state: a computational study. *IEEE Transactions on Cybernetics*, **49**, 3655–3664 (2019)

[55] HASHIMOTO, T., ELDER, C. M., OKUN, M. S., PATRICK, S. K., and VITEK, J. L. Stimulation of the subthalamic nucleus changes the firing pattern of pallidal neurons. *Journal of Neuroscience*, **23**, 1916–1923 (2003)

[56] REESE, R., LEBLOIS, A., STEIGERWALD, F., PÖTTER-NERGER, M., HERZOG, J., MEHDORN, H. M., DEUSCHL, G., MEISSNER, W. G., and VOLKMANN, J. Subthalamic deep brain stimulation increases pallidal firing rate and regularity. *Experimental Neurology*, **229**, 517–521 (2011)

[57] FOUTZ, T. J. and MCINTYRE, C. C. Evaluation of novel stimulus waveforms for deep brain stimulation. *Journal of Neural Engineering*, **7**, 066008 (2010)

[58] CONTARINO, M. F., BOUR, L. J., VERHAGEN, R., LOURENS, M. A. J., DE BIE, R. M. A., VAN DEN MUNCKHOF, P., and SCHUURMAN, P. R. Directional steering: a novel approach to deep brain stimulation. *Neurology*, **83**, 1163–1169 (2014)

[59] CHIKEN, S. and NAMBU, A. Mechanism of deep brain stimulation: inhibition, excitation, or disruption? *Neuroscientist*, **22**, 313–322 (2016)

[60] TASS, P. A. Stochastic phase resetting of two coupled phase oscillators stimulated at different times. *Physical Review E*, **67**, 051902 (2003)

[61] TASS, P. A. A model of desynchronizing deep brain stimulation with a demand-controlled coordinated reset of neural subpopulations. *Biological Cybernetics*, **89**, 81–88 (2003)

[62] HAUPTMANN, C., POPOVYCH, O., and TASS, P. A. Effectively desynchronizing deep brain stimulation based on a coordinated delayed feedback stimulation via several sites: a computational study. *Biological Cybernetics*, **93**, 463–470 (2005)

[63] POPOVYCH, O. V. and TASS, P. A. Desynchronizing electrical and sensory coordinated reset neuromodulation. *Frontiers in Human Neuroscience*, **6**, 58 (2012)

[64] LYSYANSKY, B., POPOVYCH, O. V., and TASS, P. A. Optimal number of stimulation contacts for coordinated reset neuromodulation. *Frontiers in Neuroengineering*, **6**, 5 (2013)

[65] FAN, D. and WANG, Q. Improving desynchronization of parkinsonian neuronal network via triplet-structure coordinated reset stimulation. *Journal of Theoretical Biology*, **370**, 157–170 (2015)

[66] YU, Y., HAO, Y., and WANG, Q. Model-based optimized phase-deviation deep brain stimulation for Parkinson's disease. *Neural Networks*, **122**, 308–319 (2020)

[67] CAPOZZO, A., FLORIO, T., CONFALONE, G., MINCHELLA, D., MAZZONE, P., and SCARNATI, E. Low frequency stimulation of the pedunculopontine nucleus modulates electrical activity of subthalamic neurons in the rat. *Journal of Neural Transmission*, **116**, 51–56 (2009)

[68] GARCIA-RILL, E., LUSTER, B., D'ONOFRIO, S., MAHAFFEY, S., BISAGNO, V., and URBANO, F. J. Pedunculopontine arousal system physiology — deep brain stimulation (DBS). *Sleep Science*, **8**, 153–161 (2015)

[69] WANG, J. W., ZHANG, Y. Q., ZHANG, X. H., WANG, Y. P., LI, J. P., and LI, Y. J. Deep brain stimulation of pedunculopontine nucleus for postural instability and gait disorder after Parkinson disease: a meta-analysis of individual patient data. *World Neurosurgery*, **102**, 72–78 (2017)

[70] MARTENS, H. C. F., TOADER, E., DECRÉ, M. M. J., ANDERSON, D. J., VETTER, R., KIPKE, D. R., BAKER, K. B., JOHNSON, M. D., and VITEK, J. L. Spatial steering of deep brain stimulation volumes using a novel lead design. *Clinical Neurophysiology*, **122**, 558–566 (2011)

[71] BEUTER, A., LEFAUCHEUR, J. P., and MODOLO, J. Closed-loop cortical neuromodulation in Parkinson's disease: an alternative to deep brain stimulation? *Clinical Neurophysiology*, **125**, 874–885 (2014)

[72] MIRZA, K. B., GOLDEN, C. T., NIKOLIC, K., and TOUMAZOU, C. Closed-loop implantable therapeutic neuromodulation systems based on neurochemical monitoring. *Frontiers in Neuroscience*, **13**, 808 (2019)

[73] GRANT, P. F. and LOWERY, M. M. Simulation of cortico-basal ganglia oscillations and their suppression by closed loop deep brain stimulation. *IEEE Transactions on Neural Systems and Rehabilitation Engineering*, **21**, 584–594 (2013)

[74] LITTLE, S. and BROWN, P. What brain signals are suitable for feedback control of deep brain stimulation in Parkinson's disease? *Annals of the New York Academy of Sciences*, **1265**, 9–24 (2012)

[75] POPOVYCH, O. V. and TASS, P. A. Multisite delayed feedback for electrical brain stimulation. *Frontiers in Physiology*, **9**, 46 (2018)

[76] GUO, Y. and RUBIN, J. E. Multi-site stimulation of subthalamic nucleus diminishes thalamocortical relay errors in a biophysical network model. *Neural Networks*, **24**, 602–616 (2011)

[77] DANESHZAND, M., FAEZIPOUR, M., and BARKANA, B. D. Robust desynchronization of Parkinson's disease pathological oscillations by frequency modulation of delayed feedback deep brain stimulation. *PLoS One*, **13**, e0207761 (2018)

[78] SU, F., WANG, J., NIU, S., LI, H., DENG, B., LIU, C., and WEI, X. Nonlinear predictive control for adaptive adjustments of deep brain stimulation parameters in basal ganglia-thalamic network. *Neural Networks*, **98**, 283–295 (2018)

[79] MEIDAHL, A. C., TINKHAUSER, G., HERZ, D. M., CAGNAN, H., DEBARROS, J., and BROWN, P. Adaptive deep brain stimulation for movement disorders: the long road to clinical therapy: adaptive DBS review. *Movement Disorders*, **32**, 810–819 (2017)

[80] LITTLE, S., BEUDEL, M., ZRINZO, L., FOLTYNIE, T., LIMOUSIN, P., HARIZ, M., NEAL, S., CHEERAN, B., CAGNAN, H., GRATWICKE, J., AZIZ, T. Z., POGOSYAN, A., and BROWN, P. Bilateral adaptive deep brain stimulation is effective in Parkinson's disease. *Journal of Neurology, Neurosurgery, Psychiatry*, **87**, 717–721 (2016)

[81] LITTLE, S., POGOSYAN, A., NEAL, S., ZAVALA, B., ZRINZO, L., HARIZ, M., FOLTYNIE, T., LIMOUSIN, P., ASHKAN, K., FITZGERALD, J., GREEN, A. L., AZIZ, T. Z., and BROWN, P. Adaptive deep brain stimulation in advanced Parkinson disease. *Annals of Neurology*, **74**, 449–457 (2013)

[82] VELISAR, A., SYRKIN-NIKOLAU, J., BLUMENFELD, Z., TRAGER, M. H., AFZAL, M. F., PRABHAKAR, V., and BRONTE-STEWART, H. Dual threshold neural closed loop deep brain stimulation in Parkinson disease patients. *Brain Stimulation*, **12**, 868–876 (2019)

[83] GORZELIC, P., SCHIFF, S. J., and SINHA, A. Model-based rational feedback controller design for closed-loop deep brain stimulation of Parkinson's disease. *Journal of Neural Engineering*, **10**, 026016 (2013)

[84] MASTRO, K. J., ZITELLI, K. T., WILLARD, A. M., LEBLANC, K. H., KRAVITZ, A. V., and GITTIS, A. H. Cell-specific pallidal intervention induces long-lasting motor recovery in dopamine-depleted mice. *Nature Neuroscience*, **20**, 815–823 (2017)

[85] MASTRO, K. J., BOUCHARD, R. S., HOLT, H. A. K., and GITTIS, A. H. Transgenic mouse lines subdivide external segment of the globus pallidus (GPe) neurons and reveal distinct GPe output pathways. *Journal of Neuroscience*, **34**, 2087–2099 (2014)

[86] GITTIS, A. H., BERKE, J. D., BEVAN, M. D., CHAN, C. S., MALLET, N., MORROW, M. M., and SCHMIDT, R. New roles for the external globus pallidus in basal ganglia circuits and behavior. *Journal of Neuroscience*, **34**, 15178–15183 (2014)

[87] GITTIS, A. H. and YTTRI, E. A. Translating insights from optogenetics into therapies for Parkinson's disease. *Current Opinion in Biomedical Engineering*, **8**, 14–19 (2018)

[88] LIANG, S. and WANG, Z. Controlling a neuron by stimulating a coupled neuron. *Applied Mathematics and Mechanics* (*English Edition*), **40**(1), 13–24 (2019) https://doi.org/ 10.1007/s10483-019-2407-8

[89] ZHANG, X., LIU, S., ZHAN, F., WANG, J., and JIANG, X. The effects of medium spiny neuron morphologcial changes on basal ganglia network under external electric field: a computational modeling study. *Frontiers in Computational Neuroscience*, **11**, 91 (2017)